Behaviour of photopolymerized silicate glass fibre-reinforced dimethacrylate composites subjected to hydrothermal ageing

Part II *Hydrolytic stability of mechanical properties*

K. C. KENNEDY*,‡, T. CHEN‡, R. P. KUSY*,‡,§,¶,‖
*Department of Biomedical Engineering, ‡Dental Research Center, and also §Department of Orthodontics, and ¶Curriculum in Applied and Materials Sciences, University of North Carolina, Chapel Hill, NC 275997455, USA
E-mail: rkusy@bme.unc.edu

The flexural properties and failure morphologies of dimethacrylate-copolymer composites reinforced with either S2-glass® or quartz fibres (≈ 33–66 vol%) were examined after hydrothermal ageing (0–3 mon at 37 °C). Initially the S2-glass® composites were generally stiffer and stronger than comparably reinforced quartz composites, but within 1 wk the properties of S2-glass® composites decreased by 12%–26%. The properties of quartz composites were relatively stable, except for those of composites with the least reinforcement (35 vol%), which decreased by roughly 15%. Scanning electron microscopy revealed that in all composites buckling had occurred at the site of load application. Evidence of good fibre–matrix adhesion was observed for both types of composites under all conditions. Modelling of degradation between 1 wk and 3 mon revealed that: (1) the only temporal change was a slight *increase* in the stiffness of S2-glass® composites; and (2) higher reinforcement levels reduced the retention of strength in S2-glass® composites but had the opposite effect (on both properties) for quartz composites ($p < 0.05$). For the most highly reinforced S2-glass® composites, susceptibility to degradation was offset by high initial properties; and after ageing (elastic modulus ≈ 50 GPa, strength ≈ 1.2 GPa), these composites were still, on average, approximately 25% stiffer and 50% stronger than the more hydrostable quartz counterparts. © *1998 Kluwer Academic Publishers*

1. Introduction

As medical implant materials, metals and their alloys can pose serious drawbacks, such as the release of nickel and/or other toxic ions [1, 2] and stress shielding in orthopaedic applications [1–11]. To address this, efforts have ensued to develop implantable *composites* that will not release toxic ions and which are comparable in stiffness to bone but superior in strength, i.e. with an elastic modulus, E, of about 18–20 GPa and a strength (σ) $\geqslant$ 0.2 GPa [3, 5, 6]. Composites are particularly attractive as structural implants because they can be designed to mimic the specific anisotropic behaviour of a natural structural element [7, 12].

Composites considered for implantation typically consist of a continuous matrix reinforced with a dispersed phase of either particles or fibres. Myriad matrix-reinforcement combinations have been tried, including ceramic–metal [13], carbon–carbon [3, 5, 14, 15], and bioresorbable matrices and/or fibres [1, 16–20], but fibre-reinforced polymers (FRPs) are most prevalent. While attempts have been made to reinforce polymers with good implant histories such as poly(methyl methacrylate) [17, 21–28], polyethylene [5, 29, 30], polyurethane [9], and polypropylene [31], recent interest has focused upon engineering thermoplastics such as polycarbonate, poly(ether ether ketone), and polysulphone [2, 4–11, 18, 31–38]. Carbon fibre is usually selected as the reinforcement.

One type of composite that has been overlooked as a possible orthopaedic implant material is *silicate glass* FRPs. The inherent mechanical properties of silicate glass fibre are relatively low, and both a high volume fraction of fibre, V_f, and reinforcing efficiency, ϕ, are needed to attain sufficient mechanical properties. Historically, this has not been achieved in biocompatible silicate glass FRPs [9, 22, 31–33, 37, 39–42]. Recently, however, silicate glass has been used to *photo-pultrude* high-V_f, high-ϕ, unidirectional FRPs (UFRPs) [43, 44]. The mechanical properties

‖ Author to whom all correspondence should be addressed. Fax: 919-966-3683.

are sufficient for structural orthopaedic implantation, e.g. an elastic modulus, E, and flexural strength, σ, as high as 60 GPa and 1.7 GPa, respectively [45], but the behaviour of the composites in a warm aqueous environment was unknown.

Investigations of hydrothermal ageing in implantable FRPs have demonstrated effects on mechanical properties that range from no effect [9, 11, 32], or even slight increases [39, 41, 46], to significant drops that can exceed 50% [2, 9, 10, 23, 31, 32, 38]. Plasticization of the matrix and a loss of interphase bonding are frequently reported [2, 10, 31, 38]. Flexural properties are particularly sensitive to the interfaces because they transfer internal loads via shearing stresses. Fibre surfaces are often treated with sizing agents to enhance chemical coupling with the matrix. The susceptibility of these couples to hydrothermal attack varies from system to system and is frequently a dominant factor in mechanical degradation due to hydrothermal ageing.

In this study photo-pultruded UFRPs, made with either S2-glass® fibres or quartz (fused silica) fibres, were examined in flexure to determine the effects of hydrothermal ageing on E and σ. The failure morphology was examined via scanning electron microscopy (SEM). Regression analysis was used to show that ageing time, t, and V_f affect degradation in the two types of composites differently. The behaviours are explained in terms of differing interphase-bonding characteristics.

2. Materials and methods

2.1. Preparation of composites

Composites were constructed from a thermosetting, copolymer matrix reinforced with continuous, unidirectional, silicate-glass fibres (see Table I for mechanical properties). The comonomer consisted of 2,2-*bis*[4-(2-hydroxy-3-methacryloxypropoxy)phenyl] propane (*bis*-GMA, Polysciences, Inc., Warrington, PA, USA) and triethylene glycol dimethacrylate (TEGDMA, Aldrich Chemical Co., Inc., Milwaukee, WI, USA) photo-sensitized with benzoin ethyl ether (Owens Corning Corp., Toledo, OH, USA; respective mass ratio 61/39/0.4). Reinforcing filaments (9 μm) were yarns of either S2-glass® (Owens Corning Corp., Toledo, OH, USA) or quartz (Quartz Products Co., Louisville, KY, USA) used in the as-received condition, i.e. sized by the manufacturers with proprietary organo-silane binding agents.

Round UFRP composite "wire" (0.5 mm) was produced continuously via photo-pultrusion at a linear rate of 1.27 mm s^{-1}. Complete details of the photo-pultrusion process and equipment were outlined in Part I of this study [47] and/or elsewhere [43, 44]. Altering the number of silicate glass yarns produced composites with a range of V_f levels (Table II).

TABLE I Mechanical properties of composite constituents

Composite constituent	Elastic modulus, E (GPa)	Tensile strength, σ (GPa)	Reference
S2-glass® filaments	86	4.6	[61]
Quartz filaments	78	6.0	[62]
Copolymer	2.4	0.021	[63]

TABLE II Reinforcement composition of composites studied

Reinforcement filament type	Number of yarns	Fibre volume fraction, V_f
S2-glass®	5	0.33
	7	0.46
	8	0.53
	10	0.66
Quartz	9	0.35
	12	0.47
	14	0.54
	16	0.62

2.2. Experimental procedure

2.2.1. Hydrothermal ageing

Short specimens (60 mm) were submerged in a 37 °C deionized water bath for periods of up to 3 mon. At times ranging from 2–95 d, a battery of specimens (three to six from each of the four V_f levels for a particular composite type), was removed from the bath for testing.

2.2.2. Mechanical testing

After removal from the water bath, each specimen in a battery was blotted dry and a central segment (1.27 cm) marked for identification. Four separate determinations of the diameter ($\pm$ 1.5 μm) were collected from within the central segment, at random radial orientations, using a Sony μ-mate® digital micrometer (Sony Magnescale America, Inc., Orange, CA, USA). Following the completion of these determinations for the entire battery, flexural tests were conducted in three-point bending with the central segment of each specimen positioned over a 1.27 cm span. A complete description of the testing fixture has been reported previously [48]. An Instron® Universal Testing Machine (Instron Inc., Canton, MA, USA) maintained the deflection rate at 0.1 cm min^{-1}. All tests were conducted at room temperature ($\approx$ 25 °C) within 1 h of removal of specimens from the bath. A battery of unaged specimens was tested to provide a baseline reference.

Mechanical property values were determined using classical mechanics, which are presented below for round cross-sections (d = diameter) [49]. E was calculated via Equation 1 using the span length, L, and a slope, S, that was extrapolated from the linear portion of the load–deflection curve. Equation 2 was used to calculate σ after determining the failure load, P, which was defined as the first point where a marked drop in the load was observed.

$$E = \frac{4L^3S}{3\pi d^4} \quad (1)$$

$$\sigma = \frac{8PL}{\pi d^3} \quad (2)$$

2.2.3. SEM analysis

Failure morphology was examined via SEM for randomly selected specimens of both material types, from both ends of the reinforcement spectrum, and for both the unaged and aged conditions. Specimens were mounted on a stud and coated with AuPd for 90 s using a Polaron® E5100 SEM Coating Unit (Polaron Equipment Ltd., Waterford, UK). Examination took place under an accelerating voltage of 10 keV with an JEOL® JSM-6300 SEM (JEOL USA, Inc., Peabody, MA, USA). A JEOL® UHR Camera (JEOL USA, Inc., Peabody, MA, USA) recorded selected images on Polaroid® 665 film (Polaroid Corp., Cambridge, MA, USA).

3. Results

3.1. Mechanical properties

3.1.1. Unaged materials

The mean E and σ of the unaged S2-glass® composites ranged nominally between 20 and 60 GPa and between 1.2 and 1.7 GPa, respectively, over the range of V_f levels (Tables III and IV). Values of σ were not obtained for any of the S2-glass® composites at the lowest V_f, owing to limitations of the testing fixture and/or deflections well beyond the limits implicit in Equation 2. For the quartz composites, the ranges of the means for E and σ were about 25–40 GPa and 0.7–0.8 GPa, respectively (Tables V and VI). The properties varied linearly ($p \leqslant 0.001$) with the V_f for both materials (Fig. 1) with the exception of σ for quartz, which was approximately constant.

3.1.2. Aged materials

The effects of hydrothermal ageing on mechanical properties were different for the two types of composites but similar within each composite type for the two mechanical properties (Tables III–VI).

Two time regimes were apparent for mechanical degradation in the S2-glass® composites whereby a marked 12%–26% loss of properties occurred

TABLE III Degradation behaviour of the elastic modulus, E (GPa), in S2-glass® composites

Ageing time (d)	Fibre volume fraction, V_f			
	0.33	0.46	0.53	0.66
0	20.4 ± 1.8 (5)[a]	36.7 ± 1.3 (4)	44.7 ± 6.6 (5)	58.7 ± 6.3 (5)
2	18.0 ± 0.7 [−11.9] (5)	34.0 ± 1.9 [−7.3] (4)	48.7 ± 3.8 [+8.8] (5)	56.9 ± 3.5 [−3.0] (5)
7	16.3 ± 1.3 [−20.1] (5)	30.6 ± 1.4 [−16.5] (5)	35.8 ± 2.1 [−20.0] (5)	51.2 ± 8.7 [−12.7] (5)
14	17.0 ± 2.0 [−16.8] (4)	31.2 ± 2.2 [−15.0] (4)	38.4 ± 5.2 [−14.0] (5)	48.1 ± 3.4 [−18.0] (5)
30	17.3 ± 0.9 [−15.3] (5)	29.9 ± 2.2 [−18.6] (5)	40.1 ± 2.1 [−10.3] (5)	45.6 ± 4.0 [−22.3] (5)
60	17.1 ± 3.2 [−16.2] (5)	31.4 ± 3.7 [−14.4] (5)	39.3 ± 8.1 [−12.2] (5)	49.9 ± 4.4 [−15.0] (5)
90	18.7 ± 1.4 [−8.1] (5)	32.0 ± 1.4 [−12.8] (5)	41.9 ± 4.6 [−6.3] (5)	57.8 ± 4.2 [−1.5] (5)

[a] Data are presented as a mean ± standard deviation with the sample size in parentheses. For aged materials, the per cent deviation of the mean from the unaged baseline appears in square brackets.

TABLE IV Degradation behaviour of the flexural strength, σ (GPa), in S2-glass® composites

Ageing time (d)	Fibre volume fraction, V_f			
	0.33	0.46	0.53	0.66
0	–	1.24 ± 0.03 (3)[a]	1.38 ± 0.18 (5)	1.69 ± 0.08 (4)
2	– –	0.88 ± 0.11 [−28.8] (4)	1.40 ± 0.16 [+1.5] (5)	1.57 ± 0.07 [−7.0] (5)
7	– –	1.01 ± 0.07 [−18.6] (5)	1.21 ± 0.05 [−12.2] (5)	1.25 ± 0.12 [−26.0] (5)
14	– –	1.07 ± 0.12 [−13.5] (4)	1.14 ± 0.13 [−17.4] (5)	1.34 ± 0.19 [−20.7] (5)
30	– –	1.05 ± 0.07 [−15.0] (4)	1.23 ± 0.12 [−10.8] (5)	1.20 ± 0.06 [−29.0] (5)
60	– –	0.90 ± 0.15 [−27.1] (5)	0.88 ± 0.12 [−36.6] (5)	0.85 ± 0.02 [−50.1] (5)
90	– –	1.05 ± 0.01 [−15.2] (3)	1.32 ± 0.19 [−4.2] (5)	1.41 ± 0.05 [−16.4] (5)

[a] Data are presented as a mean ± standard deviation with the sample size in parentheses. For aged materials, the per cent deviation of the mean from the unaged baseline appears in square brackets.

TABLE V Degradation behaviour of the elastic modulus, E (GPa), in quartz composites

Ageing time (d)	Fibre volume fraction, V_f			
	0.35	0.47	0.54	0.62
0	25.8 ± 4.2 (6)[a]	34.8 ± 1.4 (6)	38.3 ± 3.0 (6)	38.8 ± 5.0 (6)
2	22.4 ± 3.1 [−13.1] (6)	38.0 ± 2.5 [+9.2] (6)	36.9 ± 3.9 [−3.7] (6)	37.8 ± 5.9 [−2.7] (6)
7	22.2 ± 3.5 [−14.1] (6)	35.7 ± 4.8 [+2.5] (6)	37.9 ± 3.3 [−1.2] (6)	39.4 ± 5.2 [+1.5] (6)
12	22.4 ± 0.8 [−13.3] (4)	32.7 ± 4.1 [−6.1] (3)	35.0 ± 1.8 [−8.8] (3)	41.3 ± 6.9 [+6.4] (3)
32	20.8 ± 2.6 [−19.4] (5)	36.1 ± 2.0 [+3.6] (5)	36.3 ± 2.3 [−5.2] (5)	39.5 ± 1.7 [+1.7] (4)
60	25.7 ± 3.6 [−0.5] (5)	35.3 ± 3.8 [+1.4] (5)	36.4 ± 1.5 [−5.1] (5)	37.7 ± 4.9 [−2.7] (5)
95	18.8 ± 2.1 [−27.4] (5)	33.9 ± 1.3 [−2.6] (5)	36.2 ± 3.0 [−5.6] (5)	37.1 ± 2.2 [−4.5] (5)

[a] Data are presented as a mean ± standard deviation with the sample size in parentheses. For aged materials, the per cent deviation of the mean from the unaged baseline appears in square brackets.

TABLE VI Degradation behaviour of the flexural strength, σ(GPa), in quartz composites

Ageing time (d)	Fibre volume fraction, V_f			
	0.35	0.47	0.54	0.62
0	0.76 ± 0.08 (6)[a]	0.73.8 ± 0.14 (6)	0.81 ± 0.08 (6)	0.76 ± 0.12 (6)
2	0.58 ± 0.03 [−23.9] (6)	0.69 ± 0.06 [−6.0] (6)	0.78 ± 0.07 [−3.5] (6)	0.76 ± 0.11 [−0.5] (6)
7	0.66 ± 0.03 [−13.1] (6)	0.73 ± 0.07 [+0.2] (6)	0.78 ± 0.05 [−3.5] (6)	0.78 ± 0.07 [+2.3] (6)
12	0.61 ± 0.05 [−19.9] (4)	0.72 ± 0.04 [−0.6] (3)	0.80 ± 0.02 [−1.0] (3)	0.81 ± 0.06 [+6.6] (3)
32	0.70 ± 0.10 [−8.3] (5)	0.73 ± 0.09 [−0.3] (5)	0.79 ± 0.08 [−2.7] (5)	0.81 ± 0.15 [+6.1] (4)
60	0.74 ± 0.10 [−3.3] (5)	0.73 ± 0.06 [+0.4] (5)	0.74 ± 0.09 [−8.2] (5)	0.76 ± 0.08 [−0.8] (5)
95	0.63 ± 0.04 [−17.6] (5)	0.67 ± 0.08 [−8.3] (5)	0.73 ± 0.50 [−9.4] (5)	0.80 ± 0.13 [+4.7] (5)

[a] Data are presented as a mean ± standard deviation with the sample size in parentheses. For aged materials, the per cent deviation of the mean from the unaged baseline appears in square brackets.

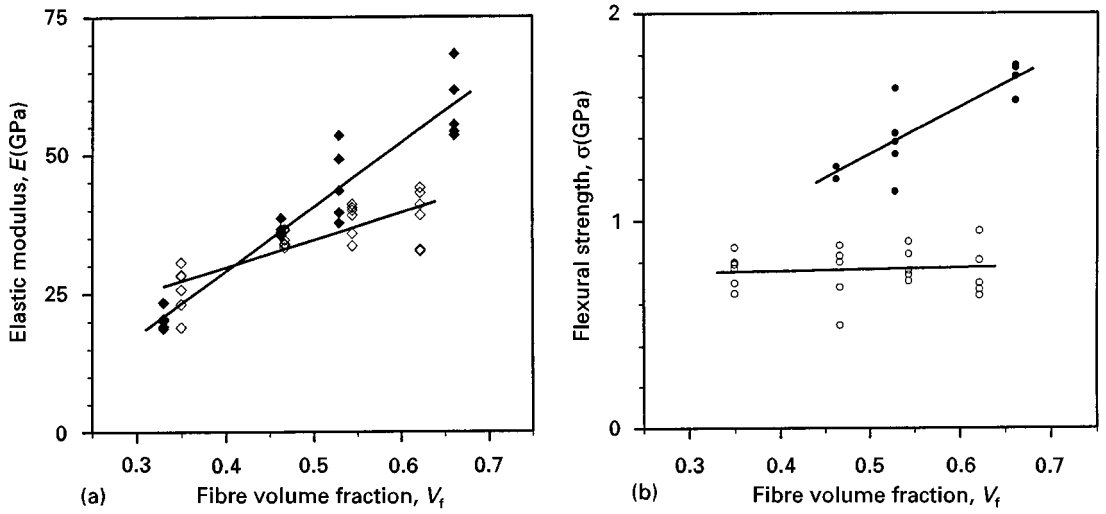

Figure 1 Flexural properties of (◆, ●) unaged S2-glass® and (◇, ○) quartz composites as a function of fibre volume fraction, V_f: (a) elastic modulus, E, and (b) flexural strength, σ. Note the relative inefficiency of reinforcement for the quartz composites, particularly with respect to σ.

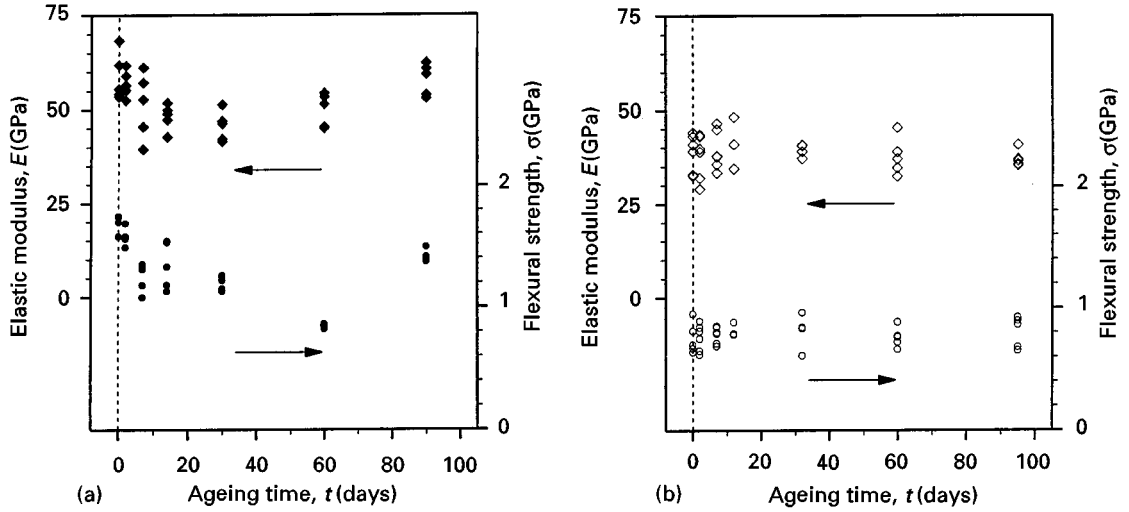

Figure 2 (◆, ◇) E and (●, ○) σ of representative composites as a function of hydrothermal ageing time, t: (a) S2-glass® ($V_f = 0.66$), and (b) quartz ($V_f = 0.62$). The dashed lines intersect the baseline data for unaged specimens. Note the lack of a pronounced transient response for the quartz composites.

within the first 7 d followed by either invariance or a less-pronounced, long-term response (Fig. 2a). For E, a slight increase from 7 d to 3 mon was noted without any apparent influence from the V_f. For σ the initial drop was followed by fluctuation about the 7 d value with a sharp drop at 60 d that was recovered by 3 mon. Additionally, for σ some indication of higher degradation was observed at the highest V_f.

For the quartz composites, deviations from the baseline properties were small (Fig. 2b) except for the composites with the lowest V_f, in which both E and σ had decreased significantly by the second day of ageing. For all levels of V_f, the long-term response consisted of fluctuations above and below a generally stable value.

Overall, for both materials the standard deviations (S.D.) of the samples of aged materials were comparable to those of the baseline samples. The values of S.D. for E ranged from about 1–9 GPa, and for σ they ranged approximately from 0.0–0.2 GPa.

3.2. SEM analysis

Composites failed by buckling at the point of load application in the central span of the specimen (Fig. 3a). The buckled regions consisted of mixed-mode failures including delamination and brittle fracture of the matrix and reinforcing fibres. All specimens revealed examples of both cleanly separated fibres (indicating a failure of the interphase boundary) and separated fibres with fractured polymer bound to the surface (indicating strong interphase bonds) (Fig. 3b–e). No morphological differences were apparent with respect to the failure sites of either unaged versus aged or high- versus low-V_f specimens.

4. Discussion

4.1. Unaged materials

The linear dependence of E and σ on the V_f (Fig. 1) can be modelled as a simplified "rule of mixtures" for UFRPs under isostrain conditions (Equation 3). The direct contributions of the matrix phase are neglected, and the property of the composite, X_c, becomes a function of the property of the reinforcing fibre, X_f, scaled by V_f and a reinforcing efficiency, φ

$$X_c = X_f V_f \varphi \quad (3)$$

Owing to the shearing stresses present in these flexural tests, φ can be considered as a measure of the performance of the interphase boundary. The φ varies with the property being measured (producing φ_E and φ_σ) and with V_f (Table VII). For all unaged materials, φ_E was relatively high (0.72–1.0), and the differences in E between the two composite types (Fig. 1a) were primarily a function of the difference in E for the two reinforcing materials (Table I). By comparison, the values for φ_σ were much lower (0.20–0.58). The materials were different with respect to the influences of V_f on φ_E and φ_σ.

4.2. Long-term ageing behaviour

To understand the differences in the long-term hydrothermal ageing behavior of the two types of composites, the degradation of both E and σ were modelled for the period following any initial transient response, i.e. from 7 d to 3 mon. Because of scatter, a simple model was selected to elucidate only the gross trends. The data were normalized by the appropriate baseline values (for example, all data for the E of aged S2-glass® composites at $V_f = 0.53$ were normalized by the mean value of E for *un*aged S2-glass® composites at that same V_f), to facilitate comparison across the range of V_f levels. Planar models (Equation 4) were regressed to the data to determine any influences that t and V_f had on the normalized elastic modulus, E_N, and flexural strength, σ_N.

$$E_N(\text{or } \sigma_N) = a + bt + cV_f \quad (4)$$

These regression analyses produced significant models ($p \leqslant 0.001$), but in each case *either* t *or* V_f was

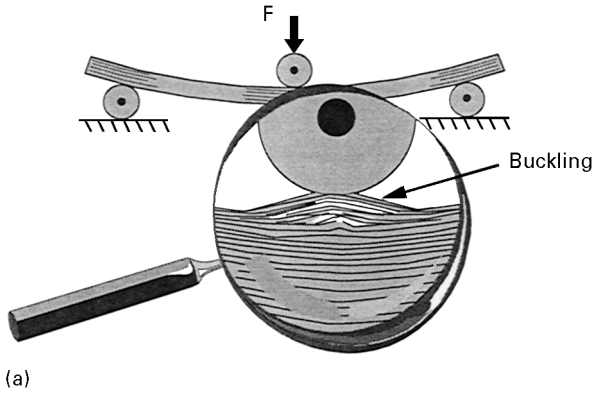

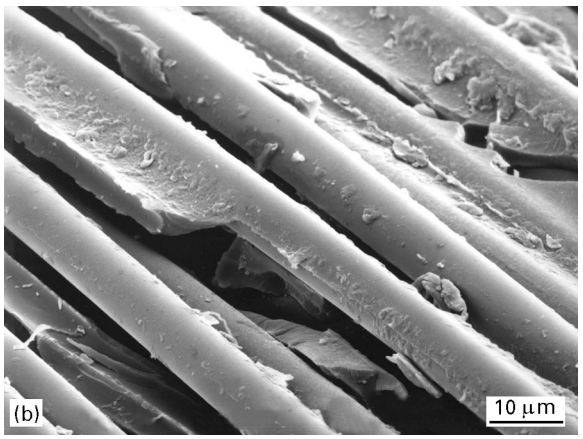

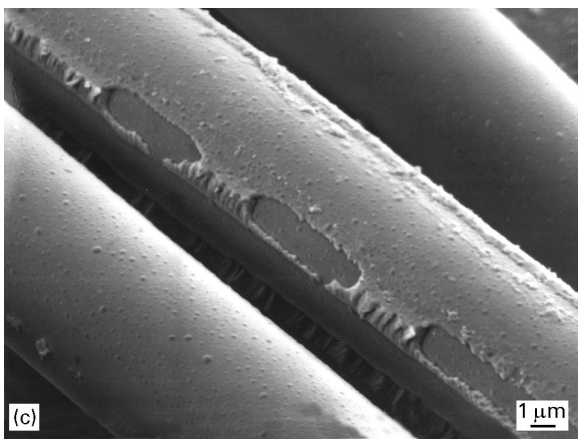

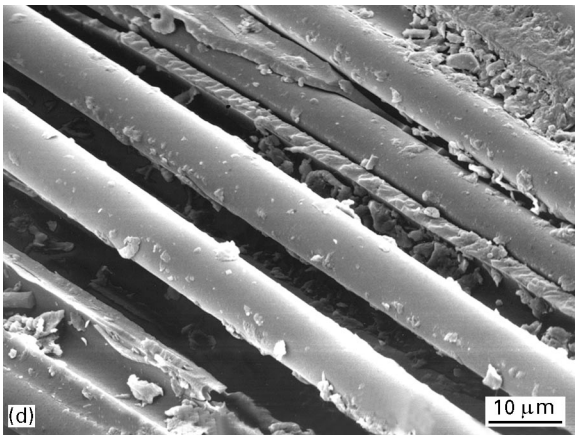

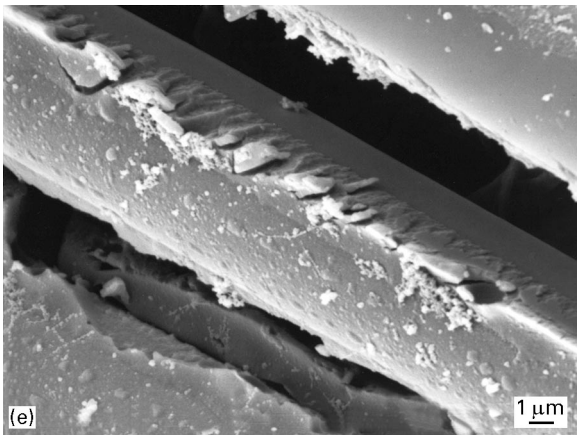

Figure 3 Failure morphology of three-point bending specimens: (a) schematic representation of gross buckling, (b, c) scanning electron micrographs of aged S2-glass® specimens, (d, e) scanning electron micrographs of aged quartz specimens. The morphology shown is representative of unaged specimens as well.

TABLE VII Reinforcing efficiency, φ, of unaged composites

Reinforcement filament type	Fibre volume fraction, V_f	Efficiency for the elastic modulus, φ_E	Efficiency for flexural strength, φ_σ
S2-glass®	0.33	0.72	–
	0.46	0.92	0.58
	0.53	0.98	0.57
	0.66	1.0	0.56
Quartz	0.35	0.95	0.36
	0.47	0.96	0.26
	0.54	0.90	0.25
	0.62	0.80	0.20

predictive, but not both (Table VIII). Because one of the two slopes of each regression plane was zero, the planes collapsed into lines and the normalized data are illustrated in two-dimensional box plots (Fig. 4), where each box (with fences and outliers) represents 18–37 data points (see Appendix, A.1) [50].

After the initial drop that occurred within the first week of ageing, the hydrothermal degradation behaviour of E in S2-glass® composites was independent of V_f (Table VIII) and increased slightly over the subsequent 11 wk period (Fig. 4a). Other reports have described increases in both the glass transition temperature and E of hydrothermally aged composites comprised of glass fibres and bisphenolic polyesters [39, 41, 46]. These reports attributed the changes to two primary phenomena: (1) a loss of trapped monomer and/or unbound low molecular weight polymer species – resulting in a *de*plasticization effect; and (2) the reaction of trapped free radicals with monomer and/or unsaturated cross-link sites within the polymer. The kinetics consisted of rapid water sorption followed by a much slower weight loss attributed to the first phenomenon. This dual character matches the degradation response observed here. Moreover, materials of the present type are known to contain both labile species that desorb with hydrothermal ageing [47, 51–54] as well as signifcant levels of unsaturation [54–60].

In the other three cases, i.e. E for quartz composites and σ for both types, after any initial degradation that

TABLE VIII Results of regression analyses for planar models describing normalized mechanical properties of composites hydrothermally aged from 7 d to 3 mon at 37 °C

Reinforcement filament type	Mechanical property	Constants of regression		
		Y-intercept	Slope for ageing time (d^{-1})	Slope for fibre volume fraction, V_f
S2-glass®	Normalized elastic modulus, E_N	0.712	0.001 11	(0.060)[a]
	Normalized flexural strength, σ_N	1.118	(− 0.000 18)	− 0.581
Quartz	Normalized elastic modulus, E_N	0.730	(− 0.000 55)	0.494
	Normalized flexural strength σ_N	0.732	(− 0.000 37)	0.495

[a] Constants shown in parentheses are not significantly different from zero ($p \geqslant 0.05$).

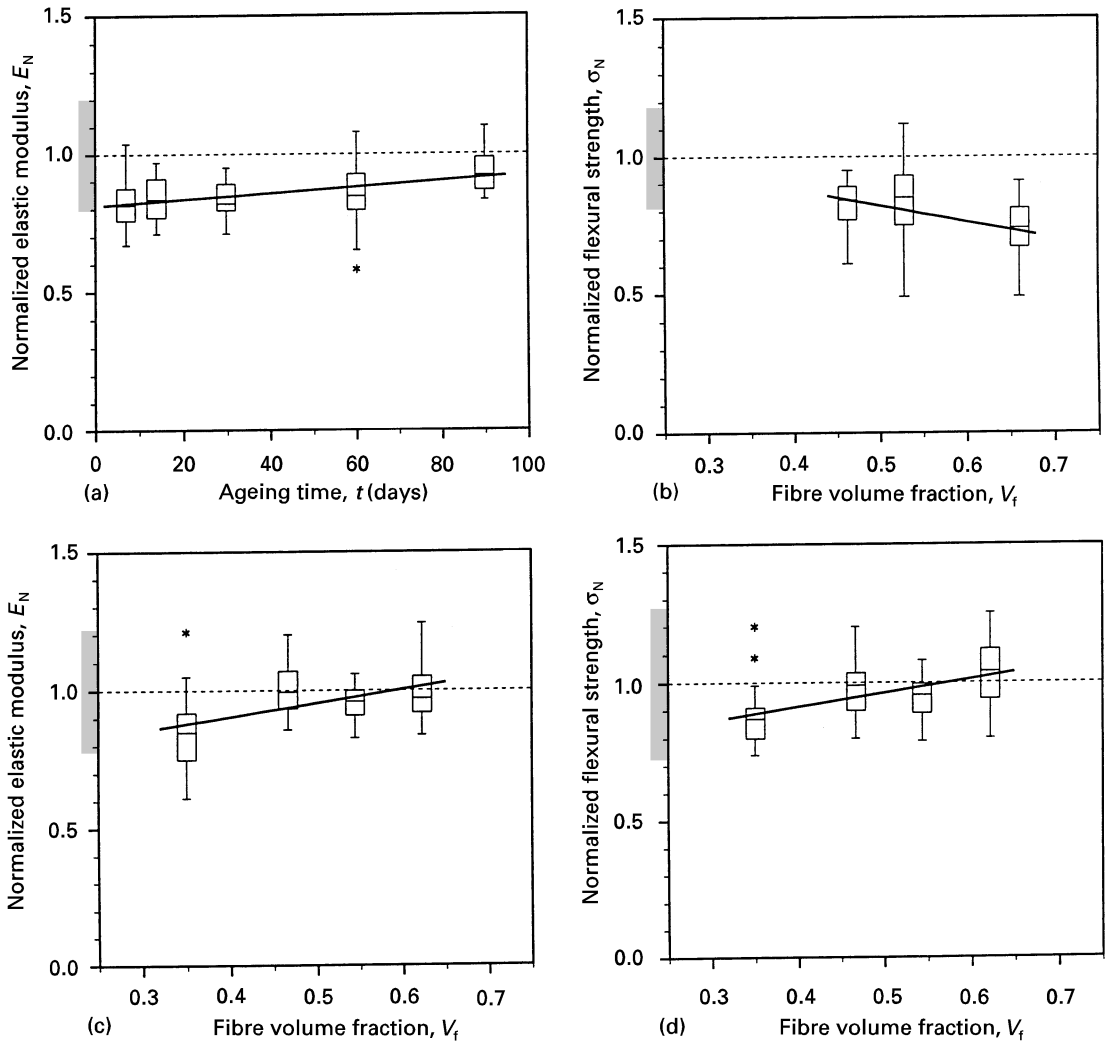

Figure 4 Normalized mechanical properties of composites hydrothermally aged from 7 d to 3 mon as a function of either t or V_f: (a, b) S2-glass®, and (c, d) quartz. In all cases the data are normalized via the mean value for unaged controls (each V_f normalized independently). According to the planar regression models (Table VIII), data for non-predictive factors were grouped together, and the regression planes collapsed into regression lines. The shaded bar along the ordinate axis of each plot represents the 95% confidence interval for the normalized, grouped, unaged controls for that plot. Note that for (a) t is the predictive factor, but in the other three cases, the V_f is the predictive factor.

occurred within the first week of ageing, t was no longer significant ($p \leqslant 0.05$) but V_f was (Table VIII, Fig. 4b–d). This trend was negative in S2-glass® composites but positive for quartz composites. This difference can be explained by the prevalence or lack of primary chemical bonds bridging the interphases. Because they transfer shear loads in flexure, the interphase boundaries may be thought of as links in a chain. If primary chemical bonds bridge the boundaries, the links are relatively brittle; and once a bond

has failed (or becomes hydrated) reformation is unlikely. However, if primary chemical bonds are less prevalent, and the principal means of stress transfer are van der Waals forces and/or internal friction, the chain, though relatively weak, exhibits ductility. For the brittle chain, increasing the V_f effectively increases the number of links. Because any chain fails when one link fails, increasing the number of links increases the probability of chain failure. For the ductile system in which weak bonds and internal friction predominate, the conformation of the reinforcing filaments may be playing a role. Because the filaments are contained in a number of lightly twisted yarns (0.5–1 turn per inch, or per 2.54 cm approximately), relative motion between individual filaments within a yarn and between adjacent yarns becomes more contorted and restricted as the average inter-fibre distance is reduced. This effect is more pronounced for the quartz composites because the numbe of filaments per yarn is approximately 40% less than for the S2-glass® yarn, and thus about two-thirds more yarns are required for an equivalent V_f (Table II). Consequently, the quartz composites contain significantly more twist, and increasig the V_f may effectively increase internal friction.

4.3. Generalized predictions based upon grouped results

To gain a concise picture of the overall hydrothermal ageing behaviour of the two materials in terms of absolute mechanical properties, the results of *all* the analyses were combined to construct an overview of degradation (Fig. 5) (see Appendix, A.2). This construction illustrates the expected behaviour of E and σ under the unaged (U) and 3 mon aged (A) conditions for two discrete levels of V_f, 0.35 and 0.65. Generally, Fig. 5 shows that the expected differences between the two materials, with respect to both the initial properties and the ageing behaviour, are most pronounced for σ and/or for the higher V_f.

At the lower V_f the predicted loss of E is 10%–20% with both materials exhibiting an E of 20–25 GPa after ageing (Fig. 5a). Differences in σ, however, are more pronounced (Fig. 5b). Although σ would decrease 15%–20% for both materials, the initial σ for

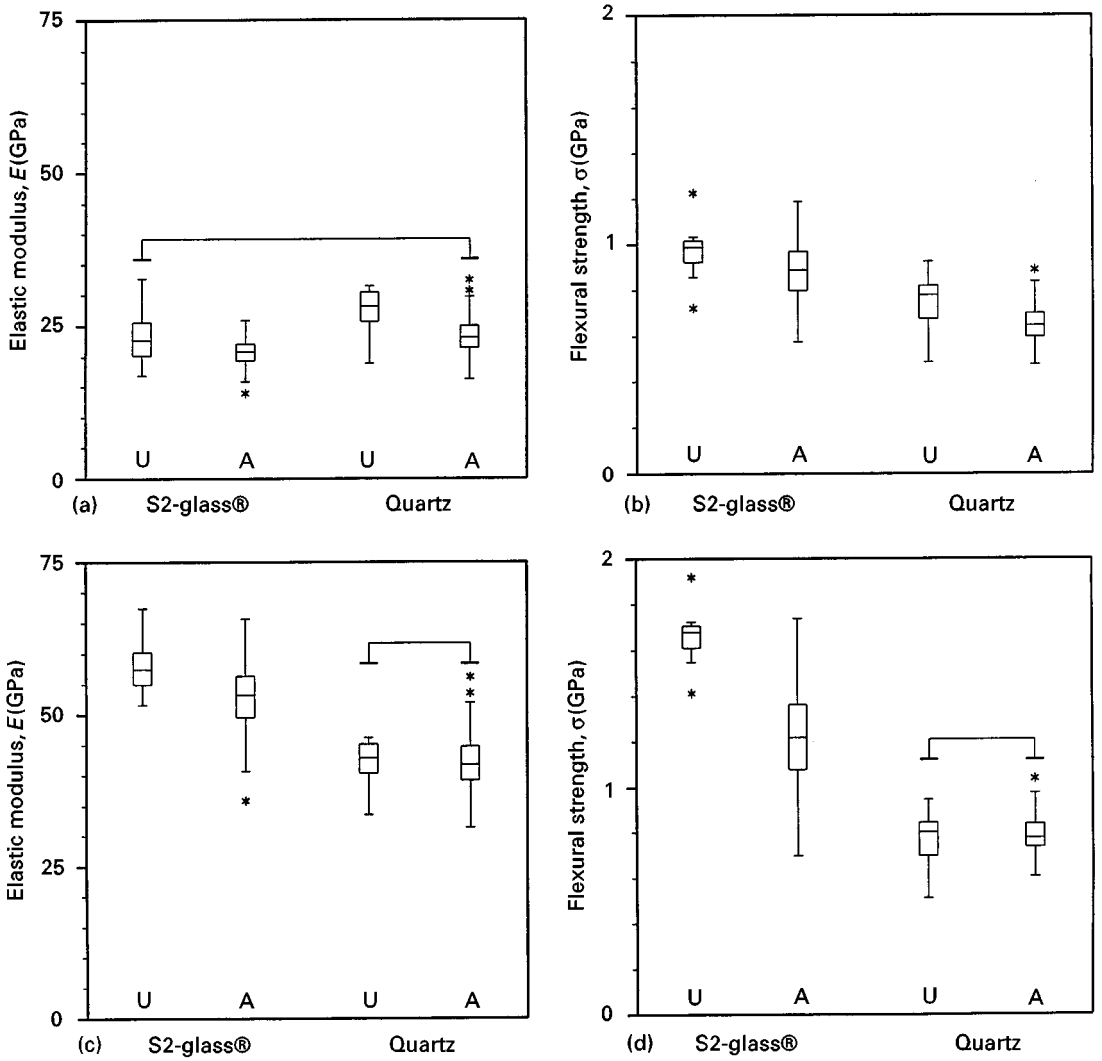

Figure 5 Predicted mechanical properties of theoretical unaged (U) and 3 mon aged (A) composites: (a, b) $V_f = 0.35$, (c, d) $V_f = 0.65$. Data boxes that are joined by an overhead bar are not statistically different from one another ($p \geqslant 0.05$), e.g. S2-glass®-U and quartz-A in (a). Note that differences between the two types of composites, with respect to both the initial property values and the ageing behaviour, are most marked for σ and/or for the high-V_f composites.

the S2-glass® composites exceeds that for quartz such that the aged S2-glass® composites (0.85 GPa) would be 15%–20% stronger than the unaged quartz composites.

At the higher V_f, the predicted behaviour of the two materials diverges more (Fig. 5c and d). The influence of V_f increases degradation for the S2-glass® composites, particularly for σ, while for the quartz materials degradation is non-existent. Nevertheless, due to differences in the fibre properties and the initial φ values, the aged S2-glass® composites ($E \approx 50$–55 GPa, $\sigma \approx 1.2$ GPa) exceed the E and σ of the more hydrostable quartz composites by about 25% and 50%, respectively.

4.4. Potential applications

Because the low-V_f composites match the E of bone (18–20 GPa) and exceed its strength ($\gg 0.2$ GPa) they might suitably be used (either directly or aggregated to form larger appliances) for load-bearing orthopaedic implantation. However, if the specific anisotropy of a natural structural element were to be emulated, e.g. for a hip prosthesis, a bi- or multi-directional reinforcement would be necessary. This could be accomplished via cross-lamination techniques [3, 4, 7, 12]. In such cases the contributions of transverse properties, which are typically relatively low, would reduce the properties of the laminate to one-half or one-third the *axial* values reported here. Of the present materials, only the high-V_f, S2-glass® composites have properties sufficient to withstand this "dilution". But even after ageing, a cross-laminated appliance of this material may exhibit an E of 17–25 GPa and a σ of 0.4–0.6 GPa.

5. Conclusion

The hydrothermal ageing of the two types of composites can be explained in terms of interphase bonding. The initial φ values and differing influences of V_f on degradation suggest that the interphase boundary in the S2-glass® composites is initially bridged by primary chemical bonds that are partly susceptible to hydrothermal degradation at 37 °C. The quartz composites may be functioning at a somewhat lower level with simpler stress transfer mechanisms dominated by secondary bonds and internal friction.

The gross failure mode in three-point bending is buckling at the site of load application, consisting of delamination and brittle fracture of the matrix and fibres. Morphological evidence of both good and poor interphase bonding is readily observable via SEM, but changes due to ageing are not.

After ageing, both types of composites maintain a significant portion of their mechanical integrity and remain relatively stable between 7 d and 3 mon. At low to moderate levels of V_f the materials are similar; and after 3 mon ageing, E and σ remain above 20 and 0.6 GPa, respectively. At higher V_f the S2-glass® composites are more susceptible to degradation, but the decreases in E and σ are more than offset by the initial properties that are much higher than those of the quartz composites. As a result the aged, high-V_f, S2-glass® composites maintain an E above 50 GPa and a σ of about 1.2 GPa, which are superior to the properties of aged, high-V_f, quartz composites by about 25% and 50%, respectively.

The composites may be useful as structural implant materials that match the compliance of bone while exceeding its strength. The low-V_f materials are appropriate for applications involving simple, unidirectional stress states. The high-V_f, S2-glass composites may be useful in the construction of multidirectionally reinforced implants, e.g. via cross-lamination, where higher axial properties are needed to counter the contributions of "off-axis" properties.

Appendix

A.1. Box plots

Each box encompasses the interquartile range (IQR) of a set of data, i.e. the 50% of the data composed of the first and third quartiles. The median is marked by a horizontal line within the box. The fences extend above and below the box to the most distant data within 1.5 IQRs of the box bounds. Data that are marked with an asterisk lie above or below the box bounds at distances between 1.5 and 3IQRs and are considered mild outliers.

A.2. Method of grouping data for generalized predictions of ageing behaviour

Predictive data were obtained by shifting and/or combining normalized data and reverting them to absolute property values. Normalized control data were grouped across levels of V_f. Normalized degradation data were shifted along the planes described by the regression equations of Table VIII to two discrete locations in the t–V_f continuum. Reversion to absolute property values was accomplished via the equations of the regression lines shown in Fig. 1.

For example, the data represented by the two boxes at the left-hand side of Fig. 5a, i.e. the predicted E for unaged (U) and 3 mon aged (A) S2-glass® composites at $V_f = 0.35$, were generated via the following procedure:

1. for U, all E_N data for *unaged* S2-glass® composites at *all* levels of V_f were combined into one group and scaled by an absolute E factor, which was predicted via the regression equation of the upper line in Fig. 1a for a $V_f = 0.35$;
2. for A, all E_N data for *aged* S2-glass® composites at *all* levels of V_f and *all* t (from 7 d to 3 mon) were shifted along the regression plane, described by the constants in the first row of Table VIII, to a common $V_f = 0.35$ and a common t of 3 mon (92 d). These data were then scaled by the same absolute E factor as described in step 1.

Acknowledgements

The authors thank the UNC-CH Department of Orthodontics for financial support and Ms Cathy

Tangen of the UNC-CH Biometrics Consulting Laboratory (under the direction of Dr Gary Koch, Department of Biostatistics) for her contributions to the statistical analysis. We also thank the Owens Corning Corporation and Quartz Products Co., for contributing the silicate-glass yarn materials.

References

1. G. O. HOFFMANN, *Arch. Orthop. Trauma. Surg.* **114** (1995) 123.
2. M. R. MEYER, R.J. FRIEDMAN, H. D. SCHUTTE Jr and R. A. LATOUR Jr, *J. Biomed. Mater. Res.* **28** (1994) 1221.
3. P. CHRISTEL, A. MEUNIER, S. LECLERCQ, Ph. BOUQUET and B. BUTTAZZONI, *J. Biomed. Mater. Res. Appl. Biomater.* **21** (1987) 191.
4. F. P. MAGEE, A. M. WEINSTEIN, J. A. LONGO, J. B. KOENEMAN and R. A. YAPP, *Clin. Orthopaed. Rel. Res.* **235** (1988) 237.
5. H. B. SKINNER, *ibid.* **235** (1988) 224.
6. L. M. WENZ, K. MERRITT, S. A. BROWN, A. MOET and A. D. STEFFEE, *J. Biomed. Mater. Res.* **24** (1990) 207.
7. F.-K. CHANG, J. L. PEREZ and J. A. DAVIDSON, *ibid.* **24** (1990) 873.
8. K. A. JOCKISCH, S. A. BROWN, T. W. BAUER and K. MERRITT, *ibid.* **26** (1992) 133.
9. A. J. GOLDBERG, C. J. BURSTONE, I. HADJINIKOLAOU and J. JANCAR, *ibid.* **28** (1994) 167.
10. R. A. LATOUR Jr and J. BLACK, *ibid.* **26** (1992) 593.
11. M. C. ZIMMERMAN, H. L. SCALZO, J. R. PARSONS, A. H. TOROP and T. S. LIN, *Biomaterials* **12** (1991) 424.
12. R. HUISKES and S. J. HOLLISTER, *J. Biomed. Engr. Trans. ASME* **115** (1993) 520.
13. W. E. COOK, C. R. MANNING Jr, J.C. HURT and D. F. TAYLOR, *J. Biomed. Mater. Res. Symp.* **2** (1972) 443.
14. G. M. JENKINS and C. J. GRIGSON, *J. Biomed. Mater. Res.* **13** (1979) 371.
15. D. ADAMS, D. F. WILLIAMS and J. HILL, *ibid.* **12** (1978) 35.
16. I. CIFKOVÁ, M. ŠTOL, R. HOLUŠA and M. ADAM, *Biomaterials* **8** (1987) 30.
17. J. S. ROMÁN and P. G. GARCÍA, *ibid.* **12** (1991) 236.
18. J. C. KNOWLES, G. W. HASTINGS, H. OHTA, S. NIWA and N. BOEREE, *ibid.* **13** (1992) 491.
19. H. ALEXANDER, A. B. WEISS and J. R. PARSONS, *Aktuelle Probleme in Chirurgie und Orthopadie* **26** (1983) 78.
20. M. A. ATTAWIA, J. DEVIN and C. T. LAURENCIN, *ACS Polym. Prepr.* **35** (1994) 840.
21. C. A. BUCKLEY, E. P. LAUTENSCHLAGER and J. L. GILBERT, in "Proceedings of the 17th Annual Meeting of the Society for Biomaterials" (Society for Biomaterials, Minneapolis, MN, 1991) p. 45.
22. D. C. SMITH, *J. Prost. Dent.* **12** (1962) 1066.
23. K. EKSTRAND, I. E. RUYTER and H. WELLENDORF, *J. Biomed. Mater. Res.* **21** (1987) 1065.
24. J. D. HENDERSON Jr, R. H. MULLARKY and D. E. RYAN, *ibid.* **21** (1987) 59.
25. B. POURDEYHIMI and H. D. WAGNER, *ibid.* **23** (1989) 63.
26. L. D. T TOPOLESKI, P. DUCHEYNE and J. M. CUCKLER, in "Proceedings of the 17th Annual Meeting of the Society for Biomaterials" (Society for Biomaterials, Minneapolis, MN, 1991) p. 48.
27. D. N. HILD and P. SCHWARTZ, *J. Mater. Sci. Mater. Med.* **4** (1993) 481.
28. T. BERGENDAL, K. EKSTRAND and U. KARLSSON, *Clin. Oral. Impl. Res.* **6** (1995) 246.
29. C. SILVERTON, A. O. ROSENBERG, R. M. BARDEN, M. B. SHEINKOP and J. O. GALANTE, *J. Bone Joint Surg.* **78-A** (1996) 340.
30. J. B. PARK and R. S. LAKES, in "Biomaterials an Introduction", 2nd Edn (Plenum Press, New York, 1992) p. 180.
31. J. JANCAR and A. T. DIBENEDETTO, *J. Mater. Sci. Mater. Med.* **4** (1993) 555.
32. J. JANCAR, A. T. DIBENEDETTO and A. J. GOLDBERG, *ibid.* **4** (1993) 562.
33. J. JANCAR, A. T. DIBENEDETTO, Y. HADZIINIKOLAU, A. J. GOLDBERG and A. DIANSELMO, *ibid.* **5** (1994) 214.
34. G. MAHARAJ, S. BLESER, K. ALBERT, R. LAMBERT, S. JANI and R. JAMISON, *Biomed. Mater. Eng.* **4** (1994) 193.
35. Y. SHONO, P. C. McAFEE, B. W. CUNNINGHAM and J. W. BRANTIGAN, *J. Bone Joint Surg.* **75-A** (1993) 1674.
36. L. CLAES, *Biomed. Technik* **34** (1989) 315.
37. A. P. PATEL, A. J. GOLDBERG and C. J. BURSTONE, *J. Appl. Biomater.* **3** (1992) 177.
38. R. A. LATOUR Jr and J. BLACK, *J. Biomed. Mater. Res.* **27** (1993) 1281.
39. A. APICELLA, C. MIGLIARESI, L. NICODEMO, L. NICOLAIS, L. IACCARINO and S. ROCCOTELLI, *Composites* **13** (1982) 406.
40. W. R. KRAUSE, S.-H. PARK and R. A. STRAUP, *J. Biomed. Mater. Res.* **23** (1989) 1195.
41. C. BASTIOLI, G. ROMANO and C. MIGLIARESI, *Biomaterials* **11** (1990) 219.
42. A. J. GOLDBERG and C. J. BURSTONE, *Dent. Mater.* **8** (1992) 197.
43. R.P. KUSY and K. C. KENNEDY, "Novel Pultruded Fiber-Reinforced Plastic and Related Apparatus and Method", US Patent filed (1994).
44. K. C. KENNEDY and R. P. KUSY, *J. Vinyl Additive Technol.* **1** (1995) 182.
45. K. C. KENNEDY, T. CHEN and R. P. KUSY, in "Advanced Composites X" (ASM International®, Materials Park, OH, 1994) p. 191.
46. Y. PAPADOGIANIS, D. B. BOYER and R. S. LAKES, *J. Biomed. Mater. Res.* **19** (1985) 85.
47. K. C. KENNEDY, T. CHEN and R. P. KUSY, *J. Mater. Sci. Mater. Med.*, in press.
48. R. P. KUSY and A. M. STUSH, *Dent. Mater.* **3** (1987) 207.
49. E. P. POPOV, "Introduction to Mechanics of Solids" (Prentice-Hall, Englewood Cliffs, NJ, 1968) pp. 183, 397.
50. R. J. SIMPSON Jr, T. A. JOHNSON and I. A. AMARA, *Am. Heart J.* **116** (1988) 1663.
51. K. INOUE and I. HAYASHI, *J. Oral Rehab.* **9** (1982) 493.
52. W. SPAHL, H. BUDZIKIEWICZ and W. GEURTSEN, *Dtsch. Zahnärztl Z.* **46** (1991) 471.
53. S. KALACHANDRA and D. T. TURNER, *J. Biomed. Mater. Res.* **21** (1987) 329.
54. F. A. RUEGGENBERG and R. G. CRAIG, *J. Dent. Res.* **67** (1988) 932.
55. E. ASMUSSEN, *Scand. J. Dent. Res.* **90** (1982) 490.
56. J. L. FERRACANE and E. H. GREENER, *J. Dent. Res.* **63** (1984) 1093.
57. *Idem., J. Biomed. Mater. Res.* **20** (1986) 121.
58. I. E. RUYTER and H. ØYSÆD, *ibid.* **21** (1987) 11.
59. K. CHUNG and E. H. GREENER, *J. Oral Rehab.* **15** (1988) 555.
60. R. NOMOTO and T. HIRASAWA, *Dent. Mater. J.* **11** (1992) 177.
61. Publication 15-PL-16154-A (Owens Corning Corp., Toledo, OH, 1993).
62. Publication 2/3/052 E (Quartz Products Co., Louisville, KY, 1991).
63. R. G. CRAIG (ed.), "Restorative Dental Materials", 6th Edn (C. V. Mosby, St. Louis, MO, 1980) p. 398.

Received 18 March
and accepted 25 September 1997